Original Research Article

Immunomodulatory and Anti-cancer Potency of Lysergol on Benzo[*a*]pyrene-induced Lung Carcinogenesis and Attenuation of Tumor Progression in Mice Model

Pharmacognosy Magazine
22(1) 99–112, 2026
© The Author(s) 2025
Article reuse guidelines:
in.sagepub.com/journals-permissions-india
DOI: 10.1177/09731296251324741
journals.sagepub.com/home/phm
Sage

Yaming Li[1], Jiayin Liu[1] and Shuang Pan[1]

Abstract

Background: Benzo[*a*]pyrene (B[a]P), a polycyclic aromatic hydrocarbon exposure, is a major public health issue globally, particularly as a result of its connection to lung cancer. Individuals exposed to higher levels of B[a]P exhibit markedly elevated risks of developing pulmonary carcinoma. Globally, pulmonary carcinoma continues to be one of the top causes of cancer-related fatalities, and mitigating B[a]P exposure is decisive for alleviating this ailment.
Objectives: The therapeutic potency of lysergol, a clavine alkaloid phytochemical, against B[a]P-triggered lung carcinoma was analyzed.
Materials and Methods: Healthy Swiss albino mice were subjected to B[a]P exposure and subsequently treated with lysergol to evaluate its effectiveness in mitigating lung cancer. We recorded body mass, lung mass, and tumor occurrence, while also quantifying immunoglobulin and tumor marker levels to assess the anti-cancer properties of lysergol. To understand its impact on B[a]P metabolism and detoxification, we measured Phase I and II enzymes. Additionally, we quantified the prognostic tumor biomarkers carcinoembryonic antigen (CEA) and cytokeratin fragment 21-1 (CYFRA 21-1) in B[a]P-treated mice, as well as inflammatory cytokines to assess the anti-inflammatory efficacy of lysergol. Mitochondrial enzyme activity and proliferating cell nuclear antigen (PCNA), nuclear factor kappa B (NF-κB), cytochrome P450 1A1 (CYP1A1), and nuclear factor erythroid 2-related factor 2 (NRF2) levels were assayed to evaluate the progression of the tumor.
Results: Lung tissue histology analysis was performed to confirm the anti-cancer effects of lysergol. Our findings revealed that both pretreatment and post-treatment with lysergol prevented tumor occurrence and regulated immunoglobulin and tumor biomarker levels in B[a]P-exposed mice. Phase I enzymes decreased significantly, while Phase II enzymes increased following lysergol treatment. Additionally, lysergol treatment led to the suppression of prognostic biomarkers CEA and CYFRA 21-1, as well as inflammatory cytokines in the B[a]P-exposed animals. The treatment also resulted in decreased mitochondrial enzyme levels, thereby helping to maintain redox balance. Furthermore, lysergol reduced PCNA, NF-κB, CYP1A1, and NRF2 levels, indicating its inhibitory effect on B[a]P-induced tumor progression. Histopathological results supported our other analyses, confirming that lysergol treatment effectively reduced carcinoma initiation and progression in B[a]P-triggered mice.
Conclusion: In conclusion, lysergol demonstrates considerable potential as an anti-cancer agent, effectively mitigating B[a]P-triggered lung carcinoma in a mouse model, and warrants further investigation for its usage as a therapeutic drug for lung cancer.

Keywords

Benzo[*a*]pyrene, lung carcinoma, phytomedicine, lysergol, tricarboxylic acid cycle, metabolizing enzymes, tumor progression

Received 13 December 2024; **accepted** 31 January 2025

Introduction

Pulmonary carcinoma is the prime cause of mortality related to cancer, accounting for approximately 25% of all cancer fatalities globally (Bray et al., 2024; Siegel et al., 2018). Increased lung cancer deaths can be attributed to factors such

[1]Department of Respiratory and Critical Care Medicine, The First Affiliated Hospital of Xi'an Medical University, Xi'an, Shaanxi, China

Corresponding author:
Jiayin Liu, Department of Respiratory and Critical Care Medicine, The First Affiliated Hospital of Xi'an Medical University, Xi'an, Shaanxi 710077, China.
E-mail: ljy1218788728@sina.com

Creative Commons Non Commercial CC BY-NC: This article is distributed under the terms of the Creative Commons Attribution-NonCommercial 4.0 License (http://www.creativecommons.org/licenses/by-nc/4.0/) which permits non-Commercial use, reproduction and distribution of the work without further permission provided the original work is attributed as specified on the SAGE and Open Access pages (https://us.sagepub.com/en-us/nam/open-access-at-sage).

as Westernized diets, decreased physical activity, and smoking (Barta et al., 2019). Key factors contributing to lung diseases include tobacco smoking, which accounts for approximately 7 million deaths each year. The likelihood of developing lung carcinoma rises with the amount and duration of smoking, while former smokers remain at a higher risk compared to non-smokers even years after quitting (Bray et al., 2018; Kuang et al., 2024). Additionally, the role of inflammation in the initiation of lung carcinoma has been well-documented (Shi et al., 2015). Chronic obstructive pulmonary disease (COPD) and other pulmonary inflammatory conditions are linked to a rise in pulmonary carcinoma incidence. It has been suggested that a persistent inflammatory environment within the lungs is a key factor in the process of tumor formation (Bozinovski et al., 2016).

Tobacco smoke is rich in benzo[*a*]pyrene (B[a]P), possessing strong carcinoma-triggering effects. The impact of tobacco smoking on lung cancer rates is significant, primarily due to the presence of polycyclic aromatic hydrocarbons such as B[a]P in both tobacco smoke and vehicle emissions (Hernandez-Boussard & Hainaut, 1998; Moorthy et al., 2015). B[a]P is recognized as a key carcinogen, where the formation of deoxyribonucleic acid (DNA) adducts plays a critical role. (Zuo et al., 2014). Furthermore, high B[a]P contact levels can cause lung inflammation, dysfunction of surfactants, and edema. B[a]P also generates reactive oxygen species in metabolism, which can trigger lipid peroxidation, reduce the activity of anti-oxidant enzymes, and cause DNA mutations—contributing factors to cancer progression (Wang et al., 2013).

Present treatments for lung cancer consist of surgery, therapies with chemicals, radiation, immunomodulators, and targeted therapy (Wang, Kong, et al., 2018; Wang, Lei, et al., 2018). Each treatment has potential side effects: surgery may involve recovery pain, chemotherapy can cause queasiness and alopecia, radiation therapy may lead to discomfort in the skin and exhaustion, targeted therapies can result in gastrointestinal issues and skin rashes, and immunotherapy might cause inflammation in various organs (Anand et al., 2022). While these treatments can enhance survival and quality of life, managing their side effects is a greater task. Pharmacological efforts to lessen the severity of side effects can be expensive, target-specific types of toxicity, and may lead to drug interactions and new side effects (Devlin et al., 2017).

Phytomedicine has been utilized for eras to address several health issues, including cancer, and 80% of the population globally depends on alternative medicine (Imtiaz et al., 2024). Advances in modern biomolecular science have enhanced understanding of herbs' anti-cancer, anti-inflammatory, and anti-viral properties (Jenča et al., 2024). Phytochemicals, biologically active compounds found in plant parts, play multiple pharmacological roles by influencing molecular pathways involved in cancer development. These compounds can boost anti-oxidant levels, deactivate carcinogens, attenuate proliferation, trigger cell cycle arrest and apoptosis, prevent carcinoma cell metastasis, and modulate the immune response (Singh et al., 2016). Herbal medicines are often regarded as natural alternatives with minimal side effects and a lower risk of dependency (Mahady, 2001). Lysergol is one such naturally occurring alkaloid derived from the ergot fungus, specifically from the species *Claviceps purpurea* and from the seeds of *Ipomoea muricata* (Matsumoto et al., 2022). Research has shown that lysergol possesses various pharmacological effects, including potential analgesic, hypotensive, neuroprotective, psychotropic (Yuan et al., 2017), anti-inflammatory, and anti-bacterial properties (Maurya et al., 2013). In this research, we examined the anti-cancer efficacy of lysergol against B[a]P-triggered pulmonary carcinoma.

Materials and Methods

Chemicals and Reagents

Lysergol (purity: 95%) was purchased from AstaTech Inc., USA. B[a]P (purity: 96%) and other chemicals were purchased from Sigma–Aldrich, USA. The commercial assay kits were procured from Abcam, USA; MyBioSource, USA; LSbio, USA; and Elabscience, USA, respectively, to determine the biochemical marker levels. In this work, all the reagents were utilized in analytical grade.

Experimental Subjects

Healthy Swiss albino mice, aged 7–8 weeks and weighing 27 ± 5 g, were used throughout the experiments. The mice were housed in a temperature-controlled facility at 25°C ± 2°C with a 12-h light/dark cycle and 35% humidity, and they had *ad libitum* access to food and drinking water. The mouse standard diet includes the total protein (14 g), total fat from soybean oil (4 g), fiber (5 g), total carbohydrate (42 g), and caloric value (3.85 kcal/g) (Bio-Serv, USA). All experimental procedures adhered to institutional guidelines, ensuring the care and welfare of the animals involved in the study.

Study Design

Animals were aggregated into four different treatment clusters. Group I, serving as the control group, was orally administered corn oil for a duration of 16 weeks. Group II animals received 50 mg/kg body weight of B[a]P, dissolved in maize oil, administered orally twice a week for the first 4 weeks. Following this initial treatment period, the Group II mice were continued with vehicle corn oil treatment for an additional 12 weeks. Group III mice were treated with lysergol at a dosage of 25 mg/kg body weight (Patil et al., 2012), also dissolved in corn oil, and given orally on a daily basis for 6 weeks. After this, these mice were treated with B[a]P twice a week for 10 weeks, mirroring the treatment schedule of Group II. For the post-initiation experiments, Group IV

animals were first administered B[a]P using the same regimen as described for Group II for a total of 6 weeks. Subsequently, they received lysergol, following the same daily dosing schedule as Group III, for a period of 10 weeks.

Twenty-four hours after the experiment concluded, the animals fasted overnight on the last day of experiments before the induction of anesthesia. Subsequently, the mice were euthanized via decapitation. Measurements were taken for body weight, lung weight, and the number of tumors. Blood samples were collected through cardiac puncture. The removed lung tissue was thoroughly rinsed with chilled saline, gently dried using filter paper, and then weighed. For biochemical analysis, lung homogenate with 0.1 M potassium phosphate buffer was used. The pulverized tissue was centrifuged at 3,500 rpm for 15 min at 4°C. The aqueous phase was harvested and utilized for further analysis. For histopathological analysis, the lung tissue was subjected to 10% formalin fixation.

Quantification of Immunoglobulin Levels

Immunoglobulin levels in the serum of pulmonary carcinoma-induced, untreated, and lysergol-treated rats were quantified using the kits purchased from Abcam. The immunoglobulins react with the immunoglobulin coated on the microtiter wells. The bound immunoglobulins were detected with horseradish peroxidase-coated anti-immunoglobulin antibodies. 3,3′,5,5′-Tetramethylbenzidine was added to quantify the enzyme bound to the immunosorbent. Intermediate washing steps were performed as per the guidelines provided in the manual. The final absorbance was measured at 450 nm, and the concentration of immunoglobulins is directly proportional to enzyme-bound immunosorbents. The quantity of immunoglobulins present in the control and experimental serum were interpolated from the standard curve.

Quantification of Tumor Markers

The enzymes—gamma-glutamyl transferase (GGT), 5′-nucleotidase (5NT), aryl hydrocarbon hydroxylase (AHH), and lactate dehydrogenase (LDH)—play various roles in the context of lung cancer, potentially serving as biomarkers for diagnosis, the prognosis of tumor metabolism and pathology; therefore, we quantified these enzymes in the serum of control and experimental rats. The GGT, 5NT, AHH, and LDH were quantified using the kits procured from MyBioSource. The assay was done according to the manufacturer's protocol.

Quantification of Phase I and II Enzymes

Phase I and II enzymes play crucial roles in the metabolism of B[a]P and the detoxification processes in the lungs. Phase I enzymes, cytochrome P450 (CytP450) enzymes, cytochrome b5 (Cyt b5), nicotinamide adenine dinucleotide phosphate hydrogen cytochrome P450 reductase (NADPH CytP450 reductase), and Phase II enzymes, glutathione *S*-transferases (GST), uridine diphosphate-glucuronosyl transferases (UDP-GT), and quinine reductase (QR), were detected in the experimental mice (Du et al., 2021). The Phase I and II enzymes were quantified using the LSBio ELISA kits.

Quantification of Prognostic Biomarkers

Prognostic biomarkers of tumor—carcinoembryonic antigen (CEA) and cytokeratin fragment 21-1 (CYFRA 21-1)—levels were quantified in the experimental mice using the ELISA kit purchased from Elabscience. The assay was performed in triplicates according to the kit guidelines.

Quantification of Inflammatory Markers

Inflammatory-stimulating cytokines—tumor necrosis factor alpha (TNF-α), interleukin 6 (IL-6), and interleukin 1 beta (IL-1β)—levels were assayed in the pulmonary carcinoma-induced untreated and lysergol-treated mice. ELISA kits procured from Abcam were used for the measurement of inflammatory cytokines.

Assessment of Mitochondrial Enzymes Activity

α-Ketoglutarate dehydrogenase (KDH) activity was quantified by observing the NAD+ reduction at 340 nm in α-KDH presence (Reed & Mukherjee, 1969). Isocitrate dehydrogenase (ICDH) activity was determined following the protocol established by King (1965). Succinate dehydrogenase (SDH) activity was measured using the Nulton-Persson and Szweda (2001) protocol, where the reduction of dichloroindophenol by sodium succinate was assessed at 600 nm. Additionally, malate dehydrogenase (MDH) levels were quantified using the approach of Mehler et al. (1948), which involved measuring the NADH oxidation in the oxaloacetate presence at 340 nm.

Assessment of Lysergol Therapeutic Efficacy

The therapeutic potency of lysergol against B[a]P-triggered pulmonary carcinoma was examined by assessing proteins, proliferating cell nuclear antigen (PCNA), nuclear factor kappa B (NF-κB), Cytochrome P450 1A1 (CYP1A1), and nuclear factor erythroid 2-related factor 2 (NRF2), which play significant roles in tumor progression and response to treatment (Bodduluru et al., 2015). MyBioSource ELISA kits were utilized for the quantification of PCNA, NF-κB, CYP1A1, and NRF2. The assay was performed in triplicates as per the manual provided in the kit.

Lung Histopathological Examination

The lung tissues excised from the experimental mice were subjected to fixation in a 10% formalin solution to maintain tissue integrity and prevent degradation. Following fixation, the tissue samples were processed for paraffin embedding, which involves dehydrating the samples through a series of alcohol solutions, clearing them with xylene, and then infiltrating them with molten paraffin wax. Paraffinized tissue was then cut into thin slices measuring approximately 5 μm in thickness using a microtome. These thin sections were then mounted onto glass slides for staining. For histopathological evaluation, hematoxylin and eosin (H&E) staining was performed. Following staining, the slides were observed under a light microscope at a magnification of 40×. Photographs of the stained slides were captured to evaluate the pathological changes in lung tissue.

Statistical Analysis

The data are presented as the mean ± standard deviation, calculated from at least three independent experiments. Statistical analysis was performed using one-way analysis of variance (ANOVA) with SPSS software (version 21.0, IBM SPSS, Armonk, NY, USA). *Post hoc* Tukey's test and correlation analysis were employed to assess differences between groups. A p value below .05 was regarded as indicative of statistical significance.

Results

Clavine Alkaloid Lysergol Prevents Tumor Occurrence in B[a]P-exposed Mice

The total body mass and the lung tissue mass of the pulmonary carcinoma untreated and lysergol-treated mice were measured, and the readings are tabulated in Table 1. B[a]P treatment pronouncedly reduced the mass of the animals, and it increased the lung organ weight, indicating the occurrence of cancer. All six B[a]P-alone-exposed mice exhibited tumor, whereas in the lysergol-pretreated group, five out of six mice exhibited tumors. Compared to pretreatment, post-treatment with lysergol significantly lowered the number of tumor incidences. The number of tumor occurrences was also comparatively lower in post-lysergol-treated mice than in pre-lysergol-treated mice. The lung mass was reduced, and body weight was enhanced in the B[a]P treated with lysergol. Post-treatment with lysergol showed a significant reduction in lung weight and an increase in body weight compared to the pretreated lysergol mice.

Clavine Alkaloid Lysergol Regulates Immunoglobulin Levels in Pulmonary Carcinoma-triggered Mice

Figure 1A illustrates the levels of immunoglobulins A, M, and G in pulmonary carcinoma-induced untreated and lysergol-treated mice. B[a]P exposure considerably diminished the IgG and IgM levels and enhanced IgA levels than the healthy control group. Lysergol treatment considerably enhanced the IgG and IgM levels and diminished the IgA levels in the B[a]P-exposed rats. Post-treatment with lysergol showed significantly enhanced IgG and IgM levels and reduced IgA levels compared to the mice pretreated with lysergol.

Clavine Alkaloid Lysergol Attenuated Tumor Biomarkers in Pulmonary Carcinoma-triggered Mice

Tumor biomarker enzymes were quantified in the experimental animals, and the results are depicted in Figure 1B. The levels of the tumor biomarkers, GGT, 5NT, AHH, and LDH, were considerably enhanced in the B[a]P-exposed untreated mice compared to the other group. Both post- and pretreatment with lysergol decreased the levels of biomarkers. Post-treatment with lysergol showed a considerable reduction in the levels of biomarkers compared to the lysergol-pretreated mice.

Table 1. Clavine Alkaloid Lysergol Prevents Tumor Incidence in B[a]P-treated Mice.

Particulars	Group I	Group II	Group III	Group IV
Body weight (g)	42.83 ± 1.59	22.47 ± 1.19*	31.46 ± 0.96**	35.07 ± 0.82**
Lung weight (mg)	247.64 ± 1.19	357.81 ± 1.39*	303.74 ± 2.57**	286.08 ± 2.43**
Tumor incidence	0	8 ± 0.17*	5 ± 0.09**	3 ± 0.01**
Total no. of tumor (per mice)	0	6 ± 0.12*	4 ± 0.73**	3 ± 0.04**

Notes: Body weight, lung weight, tumor incidence, number of tumor/mice in control, B[a]P-alone-exposed mice, lysergol-pretreatment + B[a]P-exposed mice, B[a]P exposure + lysergol post-treated mice.

*Control versus B[a]P-alone-exposed mice.

**B[a]P-alone-exposed mice versus lysergol-pretreatment + B[a]P-exposed mice, B[a]P exposure + lysergol-post-treated mice.

A p value of less than .05 was considered to reflect a statistically significant difference

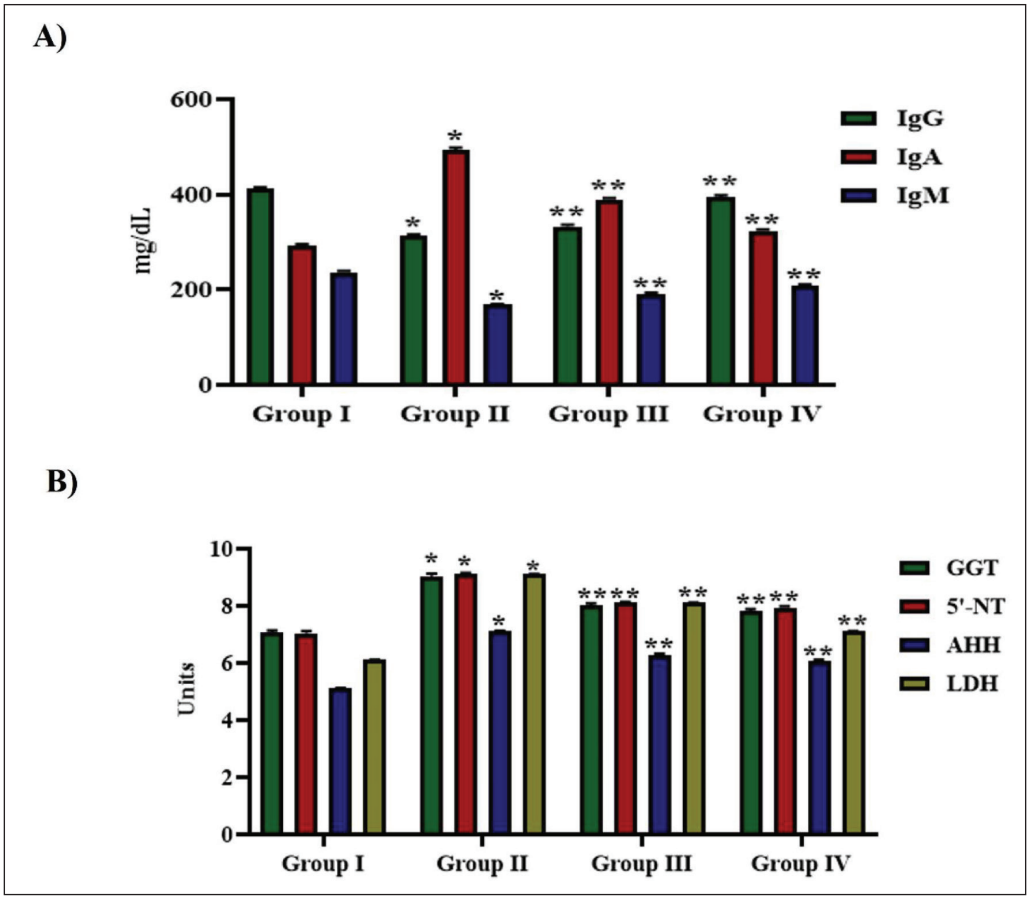

Figure 1. Clavine Alkaloid Lysergol Regulates Immunoglobulin Levels in Pulmonary Carcinoma-triggered Mice.

Notes: (A) Immunoglobulin G, immunoglobulin M, immunoglobulin G levels. (B) Tumor biomarker enzymes—gamma-glutamyl transferase (GGT), 5′-nucleotidase (5NT), aryl hydrocarbon hydroxylase (AHH), and lactate dehydrogenase (LDH)—levels in control, B[a]P-alone-exposed mice, lysergol-pretreatment + B[a]P-exposed mice, B[a]P exposure + lysergol-post-treated mice.

*Control versus B[a]P-alone-exposed mice.

**B[a]P-alone-exposed mice versus lysergol-pretreatment + B[a]P-exposed mice, B[a]P exposure + lysergol-post-treated mice.

A p value of less than .05 was considered to reflect a statistically significant difference.

Clavine Alkaloid Lysergol Normalizes Phase I and II Enzyme Levels in Pulmonary Carcinoma-triggered Mice

Phase I enzymes, which are primarily involved in the conversion of B[a]P into reactive intermediates, were quantified in the experimental animals, and the levels were represented in Figure 2A. Phase I enzymes—CytP450 enzymes, Cyt b5, and NADPH CytP450 reductase—were significantly enhanced with B[a]P exposure, whereas treatment with lysergol considerably reduced the Phase I enzymes. Post-treatment with lysergol significantly decreased the Phase I enzyme levels compared to lysergol pretreatment.

Figure 2B depicts the Phase II enzymes, GST, UDP-GT, and QR, levels in B[a]P-exposed untreated and lysergol-treated mice. The Phase II enzymes were significantly enhanced in the B[a]P-alone-exposed mice than in control and lysergol-treated mice. Pretreatment with lysergol showed considerably decreased levels of Phase II enzymes than the post-lysergol-treated mice.

Clavine Alkaloid Lysergol Inhibits Prognostic Biomarkers in Pulmonary Carcinoma-triggered Mice

Prognostic biomarkers of tumor—CEA and cytokeratin 19 fragments (CYFRA 21-1)—levels were quantified in the experiment mice, and the results are illustrated in Figure 3. A significant increase in CEA and CYFRA 21-1 levels was observed in the B[a]P-alone-exposed mice compared to the other groups. Treatment with lysergol decreased the levels of both CEA and CYFRA 21-1. Increased reduction in the levels of CEA and CYFRA 21-1 was observed in the post-lysergol-treated mice than in the lysergol-pretreated mice.

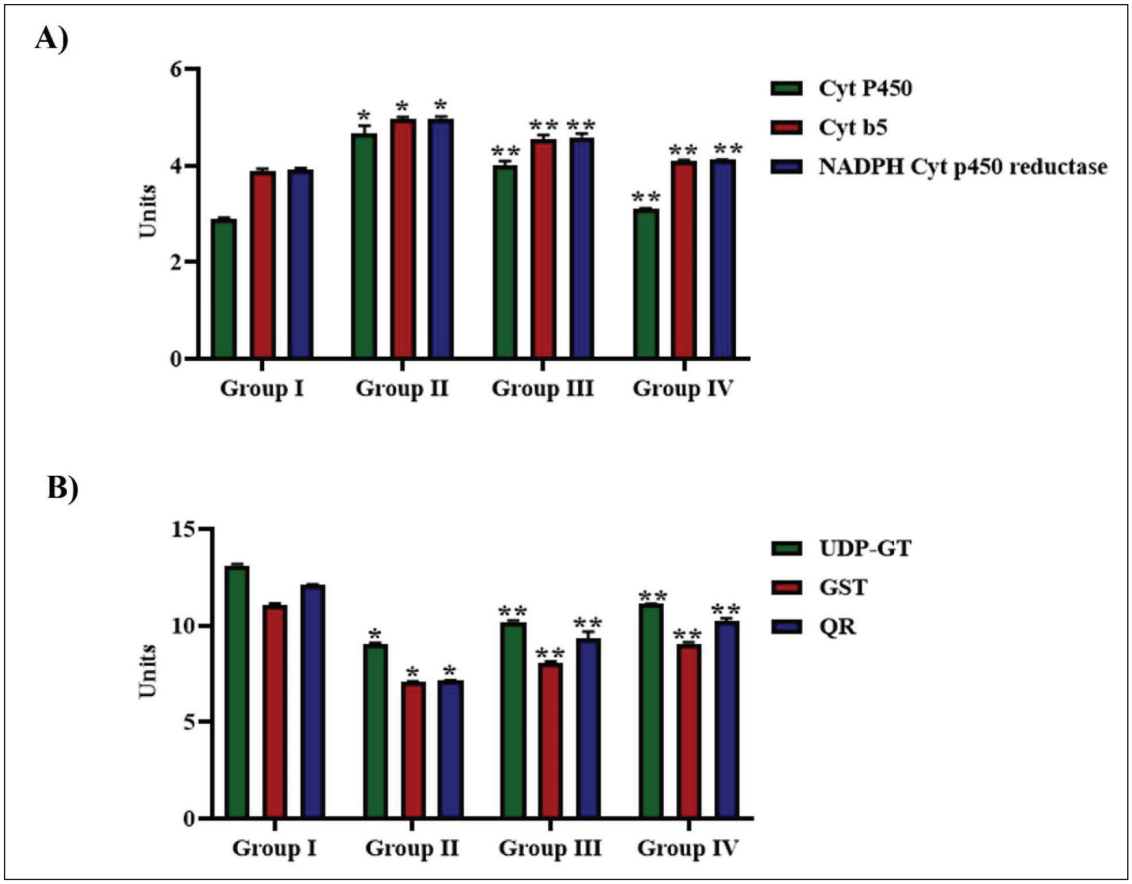

Figure 2. Clavine Alkaloid Lysergol Normalizes Phase I and II Enzyme Levels in Pulmonary Carcinoma-triggered Mice.

Notes: (A) Phase I enzymes cytochrome P450 (CytP450) enzymes, cytochrome b5 (Cyt b5), nicotinamide adenine dinucleotide phosphate hydrogen cytochrome P450 reductase (NADPH CytP450 reductase). (B) Phase II enzymes glutathione *S*-transferases (GST), uridine diphosphate-glucuronosyl transferases (UDP-GT), and quinine reductase (QR) levels in control, B[a]P-alone-exposed mice, lysergol-pretreatment + B[a]P-exposed mice, B[a]P exposure + lysergol-post-treated mice.

*Control versus B[a]P-alone-exposed mice.

**B[a]P-alone-exposed mice versus lysergol-pretreatment + B[a]P-exposed mice, B[a]P exposure + lysergol-post-treated mice.

A *p* value of less than .05 was considered to reflect a statistically significant difference.

Clavine Alkaloid Lysergol Decreases Inflammatory Cytokine Levels in Pulmonary Carcinoma-triggered Mice

Figure 4 illustrates the levels of inflammatory-stimulating cytokines in the experimental mice. Lysergol treatment considerably diminished the pro-inflammatory cytokines in B[a]P-exposed mice. The IL-1β levels, along with IL-6 and TNF-α, were considerably enhanced in B[a]P-treated mice. Post-treatment with lysergol showed a considerable reduction in inflammatory-stimulating cytokine levels than the lysergol-pretreated mice.

Clavine Alkaloid Lysergol Decreases Mitochondrial Enzyme Activities in Pulmonary Carcinoma-triggered Mice

Mitochondrial enzymes KDH, ICDH, SDH, and MDH activities were quantified in the B[a]P-exposed untreated and lysergol-treated mice. The results are illustrated in Figure 5. Mitochondrial enzymes were considerably reduced in the B[a]P than in other experimental groups. Treatment with lysergol increased the mitochondrial enzyme activity. Comparatively, post-treatment with lysergol showed a marked increase in mitochondrial enzyme activity than in the lysergol-pretreated mice.

Clavine Alkaloid Lysergol Attenuates Tumor Progression in Pulmonary Carcinoma-triggered Mice

Figure 6 depicts the levels of PCNA, NF-κB, CYP1A1, and NRF2 in B[a]P alone exposed and lysergol-treated mice. The NRF2 levels were significantly decreased with B[a]P exposure, whereas the PCNA, NF-κB, and CYP1A1 levels were increased with B[a]P exposure. Treatment with lysergol had

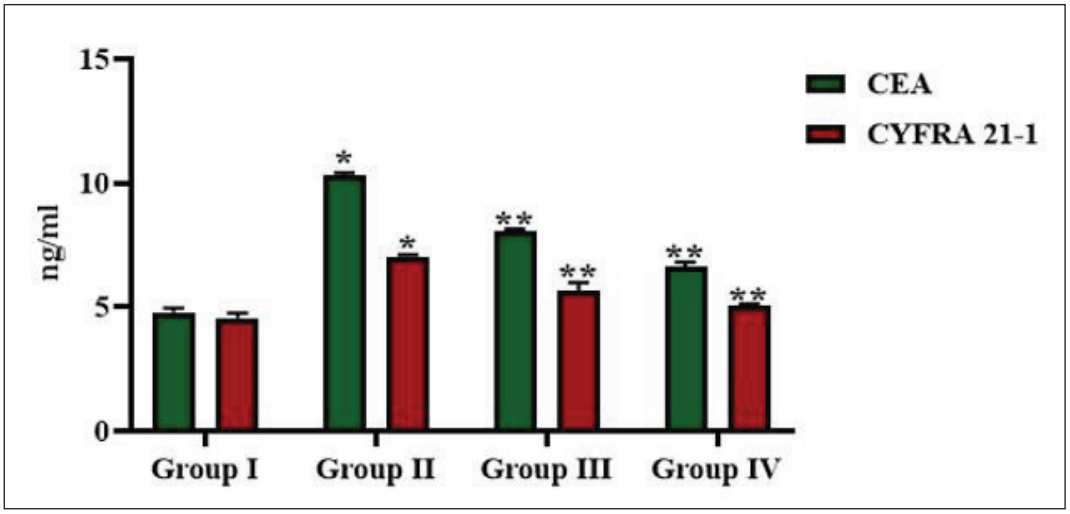

Figure 3. Clavine Alkaloid Lysergol Inhibits Prognostic Biomarkers in Pulmonary Carcinoma-triggered Mice.

Notes: Prognostic biomarkers of tumor—carcinoembryonic antigen (CEA) and cytokeratin 19 fragment (CYFRA 21-1)—levels in control, B[a]P-alone-exposed mice, lysergol-pretreatment + B[a]P-exposed mice, B[a]P exposure + lysergol-post-treated mice.

*Control versus B[a]P-alone-exposed mice.

**B[a]P-alone-exposed mice versus lysergol-pretreatment + B[a]P-exposed mice, B[a]P exposure + lysergol-post-treated mice.

A *p* value of less than .05 was considered to reflect a statistically significant difference.

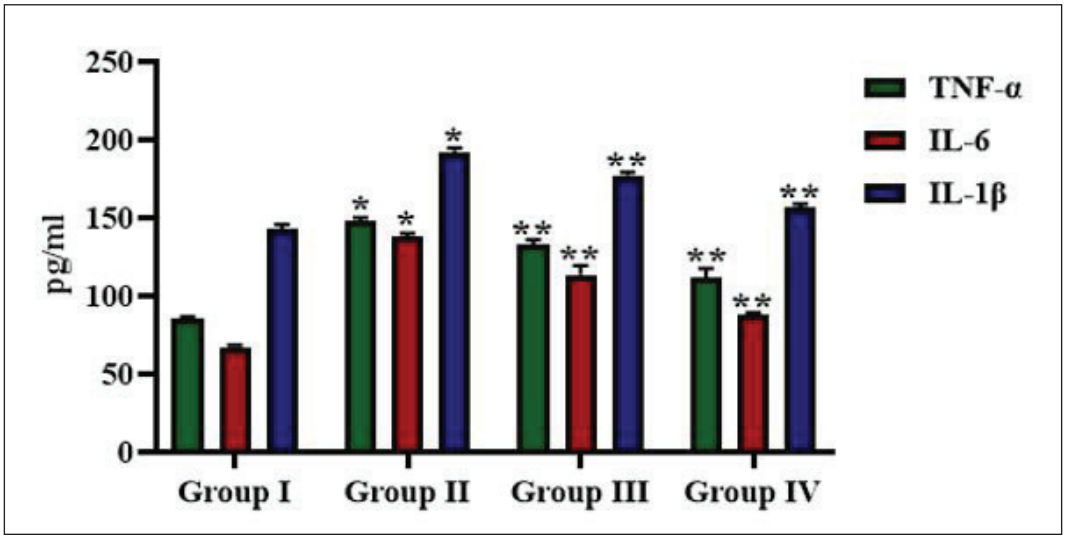

Figure 4. Clavine Alkaloid Lysergol Decreases Inflammatory Cytokine Levels in Pulmonary-carcinoma Triggered Mice.

Notes: Inflammatory stimulating cytokines tumor necrosis factor alpha (TNF-α), interleukin 6 (IL-6), and interleukin 1 beta (IL-1β) levels in control, B[a]P-alone-exposed mice, lysergol-pretreatment + B[a]P-exposed mice, B[a]P exposure + lysergol-post-treated mice.

*Control versus B[a]P-alone-exposed mice.

**B[a]P-alone-exposed mice versus lysergol-pretreatment + B[a]P-exposed mice, B[a]P exposure + lysergol-post-treated mice.

A *p* value of less than .05 was considered to reflect a statistically significant difference.

increased the NRF2 levels and decreased the PCNA, NF-κB, and CYP1A1 in B[a]P-exposed mice. Compared to the pre-treatment with lysergol, the post-treatment with lysergol showed a significant increase in NRF2 level and a reduction in PCNA, NF-κB, and CYP1A1 levels.

Clavine Alkaloid Lysergol Ameliorates B[a]P-induced Pulmonary Inflammation

The lung tissue samples from the control group exhibited thin alveolar walls, a clear tissue architecture, relatively intact

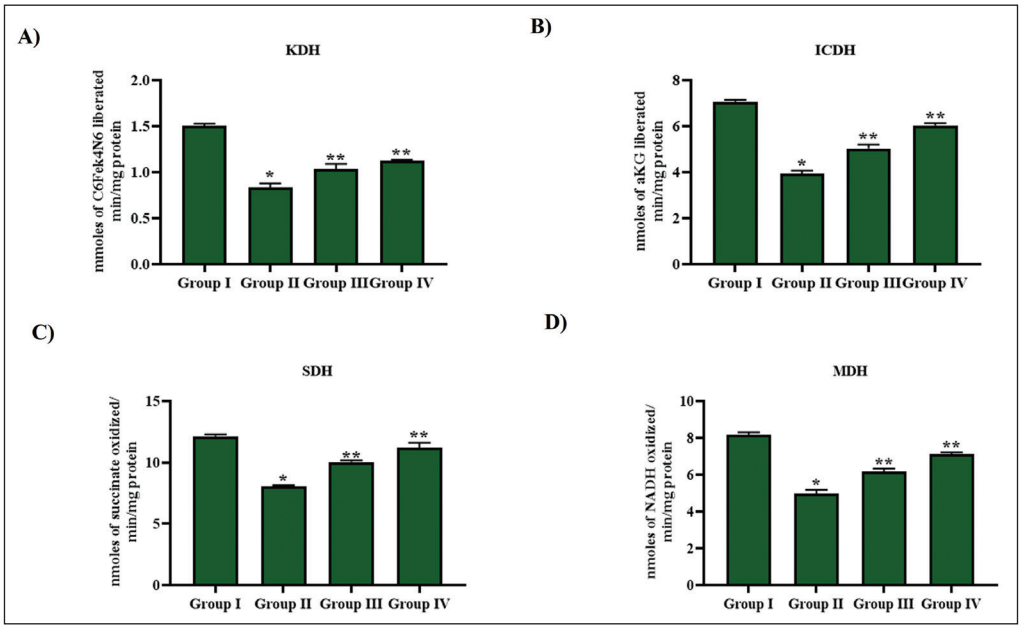

Figure 5. Clavine Alkaloid Lysergol Decreases Mitochondrial Enzymes Activities in Pulmonary Carcinoma-triggered Mice.

Notes: Mitochondrial enzymes α-ketoglutarate dehydrogenase (KDH), isocitrate dehydrogenase (ICDH), succinate dehydrogenase (SDH), and malate dehydrogenase (MDH) activities in control, B[a]P-alone-exposed mice, lysergol-pretreatment + B[a]P-exposed mice, B[a]P exposure + lysergol-post-treated mice.

*Control versus B[a]P-alone-exposed mice.

**B[a]P-alone-exposed mice versus lysergol-pretreatment + B[a]P-exposed mice, B[a]P exposure + lysergol-post-treated mice.

A *p* value of less than .05 was considered to reflect a statistically significant difference.

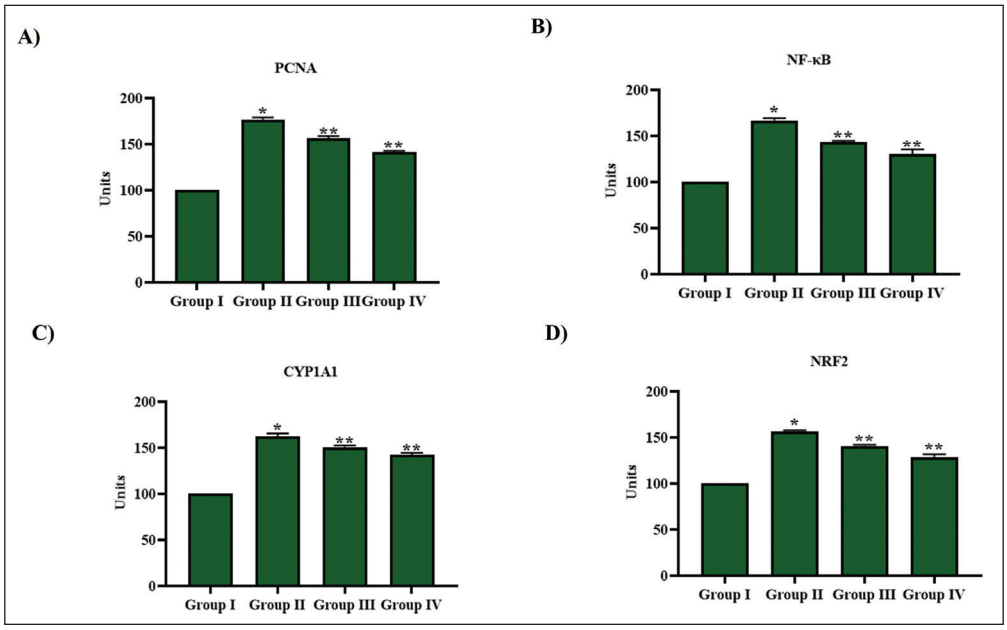

Figure 6. Clavine Alkaloid Lysergol Attenuates Tumor Progression in Pulmonary Carcinoma-triggered Mice.

Notes: Proliferating cell nuclear antigen (PCNA), nuclear factor kappa B (NF-κB), cytochrome P450 1A1 (CYP1A1), and nuclear factor erythroid-2 related factor 2 (NRF2) levels in control, B[a]P-alone-exposed mice, lysergol-pretreatment + B[a]P-exposed mice, B[a]P exposure + lysergol-post-treated mice.

*Control versus B[a]P-alone-exposed mice.

**B[a]P-alone-exposed mice versus lysergol-pretreatment + B[a]P-exposed mice, B[a]P exposure + lysergol-post-treated mice.

A *p* value of less than .05 was considered to reflect a statistically significant difference.

Table 2. Histopathological Section of Lung Tissue Injury Scores.

Individual Lung Score	Group I	Group II	Group III	Group IV
Alveolar inflammation	0.52 ± 0.12	3.7 ± 0.06*	1.7 ± 0.13**	1.4 ± 0.18**
Neutrophil infiltration	0	1.6 ± 0.08*	1.4 ± 0.08**	1.2 ± 0.01**
Peribronchiolar inflammation	0.6 ± 0.24	3.7 ± 0.14*	1.3 ± 0.02**	0.9 ± 0.01**
Enlargement of alveolar spaces	0.2 ± 0.1	1.7 ± 0.47*	1.1 ± 0.09**	0.8 ± 0.03**

Notes: Lung tissue injury scores in control, B[a]P-alone-exposed mice, lysergol-pretreatment + B[a]P-exposed mice, B[a]P exposure + lysergol-post-treated mice.

*Control versus B[a]P-alone-exposed mice.

**B[a]P-alone-exposed mice versus lysergol-pretreatment + B[a]P-exposed mice, B[a]P-exposure + lysergol-post-treated mice.

A p value of less than .05 was considered to reflect a statistically significant difference.

capillary walls, and no apparent rupture or bleeding of the alveolar walls. In contrast, the group exposed to B[a]P alone displayed significant thickening of the alveolar septa, marked interstitial congestion and edema, reduced alveolar clearance, disorganization of tissue structure, and increased inflammatory cell infiltration. The group that received pretreatment with lysergol showed only mild congestion and edema, along with minimal inflammatory-cell presence in the lung tissue. Furthermore, the group treated with lysergol after exposure demonstrated even fewer inflammatory cells and less alveolar thickening compared to the group that was pretreated with lysergol (Table 2).

Discussion

Chemotherapy is a key approach in cancer treatment, but many patients eventually develop acquired resistance, leading to treatment failure primarily due to metastasis and therapeutic resistance (Kryczka et al., 2021). This study explores the potential of natural compounds as viable alternatives for cancer treatment. Plant-derived pharmacological agents have demonstrated therapeutic potency in both the management and cancer inhibition (Choi et al., 2011; Elumalai et al., 2012). There is a growing interest in using herbal and plant-based medicines as complementary therapies, given their capacity to hinder disease progression, including carcinoma (Costea et al., 2018). Active compounds from medicinal plants modulate various biological activities that contribute to disease management, offering benefits through mechanisms such as epigenetic modifications, regulation of antioxidant enzyme activities, and alterations in metabolic signaling pathways (Pratheeshkumar et al., 2012; Ratovitski et al., 2017). Additionally, various phytocompounds are being explored in human studies as adjuncts to traditional anti-tumor therapies to alleviate adverse side effects (Rostock et al., 2011). The advantages of these alternative therapies include lower costs, fewer side effects, and broader availability (Arumugam et al., 2019). We investigated the potency of the clavine alkaloid lysergol in inhibiting cancer initiation and progression in B[*a*]P-induced lung carcinoma mice model.

Lysergol effectively inhibited the tumor occurrence in B[a]P-exposed mice and increased the body mass of the animals. A primary cause of this weight loss is tumor-induced anorexia–cachexia in the animals (Huang et al., 2019). Lysergol treatment prevented tumor incidence, thereby attenuating skeletal muscle and adipose tissue loss in B[a]P-triggered mice. Further, to assess the anti-cancer mechanism of lysergol, we analyzed the impact of lysergol on immunoglobulins. The humoral immune system is thought to play a significant role in both promoting and attenuating carcinogenesis (Peppas et al., 2020). Immunoglobulin isotype levels in cancer patients may influence tumor progression and could provide insights for early cancer detection and patient survival predictions (Carneiro et al., 2021; Sharonov et al., 2020). Additionally, the immunomodulatory effects of targeted anti-cancer treatments can arise from their direct interactions with cancer cells, as well as their capacity to modify immune cell function (Galluzzi et al., 2015).

IgG is the predominant antibody in the bloodstream and exhibits a crucial impact on the immune response to tumors. It neutralizes toxins and viruses, opsonizes pathogens, and activates complement pathways, leading to cell lysis. IgM is the initial antibody synthesized in response to a foreign body. Enhanced levels of IgM have been associated with certain malignancies, and its presence can indicate an acute immune response to the tumor (Rajendran et al., 2013). IgA is the predominant immunoglobulin found in mucosal tissues, where it plays an essential role in defending against pathogens and regulating mucosal immunity (Bertrand et al., 2023). Lysergol treatment effectively mitigated the immunosuppressive effect triggered by B[a]P. It eventually enhanced the IgG and IgM levels and diminished the IgA in B[a]P-exposed mice.

Enhanced secretion of GGT is linked to oxidative stress and inflammation in cancer, particularly in lung cancer, where high GGT levels may signify poor prognosis and tumor burden (Wei et al., 2020). Similarly, changes in 5NT activity are associated with altered purine metabolism in the tumor microenvironment, potentially impacting tumor growth and immune evasion (Corbelini et al., 2015). AHH plays a role in metabolizing known carcinogens, such as those found in tobacco smoke, and increased AHH activity may indicate

exposure to these cancer-promoting substances, contributing to lung cancer susceptibility (Kolluri et al., 2017). LDH levels are often elevated in lung cancer due to heightened glycolytic activity, correlating with tumor aggressiveness and serving as a prognostic indicator of tissue hypoxia and cellular turnover (Koukourakis et al., 2003). B[a]P exposure enhanced the tumor markers GGT, 5NT, AHH, and LDH, signifying its carcinogenic effect, whereas treatment with lysergol considerably decreased the tumor biomarkers.

Phase I enzymes, primarily consisting of CytP450 enzymes, perform a key role in the oxidation of xenobiotics, converting them into reactive forms that bind to DNA and induce mutations, as exemplified by the metabolism of B[a]P into harmful DNA adducts. Phase II enzymes facilitate the detoxification of reactive metabolites produced by Phase I enzymes, increasing their water solubility. Phase II enzymes also possess antioxidant properties that protect against oxidative stress, contributing to cancer development (Mota et al., 2015). B[a]P exposure increased the Phase I metabolizing enzymes CytP450, Cytb5, and NADPH CytP450 reductase and decreased the Phase II metabolizing enzymes UDP-GT, GST, and QR. Treatment with lysergol decreased the Phase I enzymes and enhanced the Phase II enzymes, thereby enhancing the detoxification of B[a]P and preventing tumor occurrence in mice.

CEA and cytokeratin-19 fragments (CYFRA 21-1) have been studied for their prognostic and predictive value in non-small cell lung cancer (NSCLC) patients undergoing chemotherapy. Both markers are recognized for their sensitivity and utility in diagnosis, prognosis, and treatment monitoring (Jung et al., 2011). Studies indicate that elevated levels of CEA and CYFRA 21-1 can significantly predict treatment sensitivity and survival outcomes, particularly in gefitinib-treated patients (Dal Bello et al., 2019; Okamura et al., 2013). CEA, a serum glycoprotein, is commonly considered a marker for various cancers, including colorectal, breast, and lung cancer, with increased levels often seen in smokers and in non-cancerous circumstances (Stockley et al., 1986). CYFRA 21-1, derived from cytokeratin 19, is notably enhanced in carcinoid tumors and squamous cell carcinoma of the lung, correlating with tumor size, lymph node involvement, and disease stage (Molina et al., 1994; Sertić Milić et al., 2015). Treatment with lysergol reduced levels of both CEA and CYFRA 21-1 in mice exposed to B[a]P, demonstrating its effectiveness in mitigating lung carcinoma.

A key aspect of cancer induction is tumor-promoting inflammation. Inflammation serves as a protective response aimed at eliminating harmful substances and restoring tissue homeostasis (Hanahan, 2022; Zhang, Tornmalm, et al., 2017; Zhang, Zhu, et al., 2017). However, inflammation associated with tumors typically persists over time. This ongoing inflammation can initiate or enhance anti-apoptotic signals, thereby increasing the risk of lung cancer. Furthermore, it facilitates angiogenesis, the formation of new blood vessels that supply vital nutrients to tumor cells (Tan et al., 2021). B[a]P-exposed mice exhibited considerable enhancement of inflammatory-stimulating cytokines TNF-α, IL-6, and IL-1β, whereas treatment with lysergol rendered inflammatory-attenuating effect, decreasing the levels of inflammatory-stimulating cytokines in B[a]P-exposed mice.

KDH performs a significant role in the tricarboxylic acid (TCA) cycle by converting 2-oxoglutarate to succinyl-CoA; alterations in KDH activity can disrupt cellular metabolism and energy production, potentially fostering tumor development. ICDH facilitates the conversion of isocitrate to α-ketoglutarate while generating NADPH, which is essential for maintaining redox balance; mutations in IDH can lead to the accumulation of oncometabolites, affecting metabolic signaling and increasing oxidative stress (Kamaraj et al., 2011; Selvendiran et al., 2005). SDH, part of the mitochondrial electron transport chain, oxidizes succinate to fumarate, and its dysfunction can cause succinate buildup, enhancing hypoxic signaling and stabilizing hypoxia-inducible factors (HIFs), which in turn promotes angiogenesis and cancer cell proliferation in lung cancer (Naveenkumar et al., 2013). MDH interconverts malate and oxaloacetate and reduces NAD+ to NADH, supporting the TCA cycle and gluconeogenesis; alterations in MDH activity can enhance the metabolic flexibility of cancer cells, enabling them to adapt and thrive under varying nutrient conditions, a characteristic seen in lung cancer (Zhang, Tornmalm, et al., 2017; Zhang, Zhu, et al., 2017). Treatment with lysergol increased the levels of mitochondrial enzymes KDH, ICDH, SDH, and MDH, thereby preventing oxidative stress-induced tumor initiation in B[a]P-exposed mice.

PCNA is a key biomarker of cell proliferation, playing a vital role in DNA replication and repair; elevated PCNA levels in lung cancer are linked to increased tumor growth and poor prognosis, making it a potential diagnostic marker (Wang, Kong, et al., 2018; Wang, Lei, et al., 2018). NF-κB is a transcription factor that regulates genes related to inflammation, survival, and cell proliferation; its aberrant activation in lung cancer promotes an inflammatory microenvironment conducive to tumor progression and metastasis, presenting a target for therapeutics (Rasmi et al., 2020). CYP1A1 metabolizes carcinogens such as polycyclic aromatic hydrocarbons from tobacco smoke into active metabolites that can damage DNA; increased CYP1A1 expression is related to lung cancer threat, especially among smokers (Jia et al., 2023). NRF2 regulates antioxidant proteins and detoxifying enzymes, safeguarding cells from oxidative stress; however, its dysregulation in lung cancer can facilitate tumor development and is often linked to chemotherapy resistance and unfavorable clinical outcomes (Zimta et al., 2019). Lysergol treatment decreased the levels of PCNA, NF-κB, and CYP1A1, thereby preventing tumor progression induced by B[a]P in lung carcinoma tissue. It also increased NRF2 levels and protected the lung tissue from B[*a*]P-triggered oxidative stress. These results align with our histopathological analysis of lung tissue, which revealed that treatment with lysergol resulted in

reduced inflammation compared to the untreated group exposed to B[a]P. Throughout the experiment, mice that received post-treatment with lysergol demonstrated a greater ameliorative effect than those pretreated with lysergol. In addition to these key findings, the present study has some limitations, such as it lacks in-depth molecular works to precisely understand the therapeutic roles of lysergol at the cellular level in mitigating B[a]P-induced lung cancer.

While our study yields significant insights, we acknowledge that it also has some limitations, notably the absence of in-depth molecular investigations that would provide a more precise understanding of lysergol's therapeutic mechanisms at the cellular level in counteracting B[a]P-induced lung cancer. We plan to address this limitation in our future studies, where we will prioritize detailed molecular analyses to elucidate the precise cellular and molecular mechanisms underlying lysergol's anti-cancer effects, thereby providing a more comprehensive understanding of its therapeutic potential.

Conclusion

To conclude, our study emphasizes the significant therapeutic efficacy of lysergol in mitigating B[a]P-triggered lung carcinoma in a mouse model. The findings demonstrate that lysergol treatment not only reduces tumor incidence and progression but also positively influences various biomarkers associated with cancer and inflammation. By regulating the activity of Phase I and II enzymes, suppressing key tumor markers, and maintaining redox balance, lysergol exhibits a multifaceted approach to counteracting the injurious effects of B[a]P exposure. These promising results propose that lysergol could be a valuable contender for further analysis and development as a healing agent for lung cancer, emphasizing the need for continued exploration of its mechanisms and efficacy in clinical settings.

Abbreviations

AHH: Aryl hydrocarbon hydroxylase; B[a]P: Benzo[*a*]pyrene; CEA: Carcinoembryonic antigen; CYFRA 21-1: Cytokeratin 19 fragment; CYP1A1: Cytochrome P450 1A1; Cyt b5: Cytochrome b5; CytP450: Cytochrome P450; GGT: Gamma-glutamyl transferase; GST: Glutathione *S*-transferases; ICDH: Isocitrate dehydrogenase; IL-1β: Interleukin 1 beta; IL-6: Interleukin 6; KDH: α-Ketoglutarate dehydrogenase; LDH: Lactate dehydrogenase; MDH: Malate dehydrogenase; NADPH: Nicotinamide adenine dinucleotide phosphate hydrogen; NF-κB: Nuclear factor kappa B; NRF2: Nuclear factor erythroid 2-related factor 2; NSCLC: Non-small cell lung cancer; PCNA: Proliferating cell nuclear antigen; QR: Quinine reductase; ROS: Reactive oxygen species; SDH: Succinate dehydrogenase; TCA: Tricarboxylic acid; TNF-α: Tumor necrosis factor alpha; UDP-GT: Uridine diphosphate-glucuronosyl transferases; 5NT: 5′-Nucleotidase.

Declaration of Conflicting Interests

The authors declared no potential conflicts of interest with respect to the research, authorship, and/or publication of this article.

Ethical Approval

This work has been approved by the Institutional Animal Ethical Committee by the Department of Respiratory and Critical Care Medicine, The First Affiliated Hospital of Xi'an Medical University, Xi'an, Shaanxi 710077, China.

Funding

The authors received no financial support for the research, authorship, and/or publication of this article.

Informed Consent

Not applicable.

ORCID iD

Jiayin Liu https://orcid.org/0009-0006-6138-0037

References

Anand, U., Dey, A., Chandel, A. K. S., Sanyal, R., Mishra, A., Pandey, D. K., De Falco, V., Upadhyay, A., Kandimalla, R., Chaudhary, A., Dhanjal, J. K., Dewanjee, S., Vallamkondu, J., & Pérez de la Lastra, J. M. (2023). Cancer chemotherapy and beyond: Current status, drug candidates, associated risks and progress in targeted therapeutics. *Genes and Diseases*, *10*(4), 1367–1401. https://doi.org/10.1016/j.gendis.2022.02.007

Arumugam, P., Arunkumar, K., Sivakumar, L., Murugan, M., & Murugan, K. (2019, June 15). Anticancer effect of fucoidan on cell proliferation, cell cycle progression, genetic damage and apoptotic cell death in HepG2 cancer cells. *Toxicology Reports*, *6*, 556–563. https://doi.org/10.1016/j.toxrep.2019.06.005

Barta, J. A., Powell, C. A., & Wisnivesky, J. P. (2019, January 22). Global epidemiology of lung cancer. *Annals of Global Health*, *85*(1), 8. https://doi.org/10.5334/aogh.2419

Bertrand, Y., Sánchez-Montalvo, A., Hox, V., Froidure, A., & Pilette, C. (2023, March 1). IgA-producing B cells in lung homeostasis and disease. *Frontiers in Immunology*, *14*, Article 1117749. https://doi.org/10.3389/fimmu.2023.1117749

Bodduluru, L. N., Kasala, E. R., Barua, C. C., Karnam, K. C., Dahiya, V., & Ellutla, M. (2015, December 5). Antiproliferative and antioxidant potential of hesperetin against benzo(a) pyrene-induced lung carcinogenesis in Swiss albino mice. *Chemico-Biological Interactions*, *242*, 345–352. https://doi.org/10.1016/j.cbi.2015.10.020

Bozinovski, S., Vlahos, R., Anthony, D., McQualter, J., Anderson, G., Irving, L., & Steinfort, D. (2016). COPD and squamous cell lung cancer: Aberrant inflammation and immunity is the common link. *British Journal of Pharmacology*, *173*(4), 635–648. https://doi.org/10.1111/bph.13198

Bray, F., Ferlay, J., Soerjomataram, I., Siegel, R. L., Torre, L. A., & Jemal, A. (2018, November). Global cancer statistics 2018: GLOBOCAN estimates of incidence and mortality worldwide for 36 cancers in 185 countries. *CA: A Cancer Journal for Clinicians*, *68*(6), 394–424. https://doi.org/10.3322/caac.21492

Bray, F., Laversanne, M., Sung, H., Ferlay, J., Siegel, R. L., Soerjomataram, I., & Jemal, A. (2024, May–June). Global cancer statistics 2022: GLOBOCAN estimates of incidence and mortality worldwide for 36 cancers in 185 countries. *CA:*

A Cancer Journal for Clinicians, *74*(3), 229–263. https://doi.org/10.3322/caac.21834

Carneiro, B. G. M. C., Petroianu, A., Machado, J. A. N., Anjos, Dos, P. M., F., da Silva, F. R., Alberti, L. R., Resende, V., & Barrientos, S. C. (2021, September 13). Clinical and immunological allergy assessment in cancer patients. *Scientific Reports*, *11*(1), Article 18110. https://doi.org/10.1038/s41598-021-97200-y

Choi, W.-H., Chu, J.-P., Jiang, M.-H., Baek, S.-H., & Park, H. D. (2011). Effects of fraction obtained from Korean Corni Fructus extracts causing anti-proliferation and p53-dependent apoptosis in A549 lung cancer cells. *Nutrition and Cancer*, *63*(1), 121–129. https://doi.org/10.1080/01635581.2010.516475

Corbelini, P. F., Figueiró, F., das Neves, G. M., Andrade, S., Kawano, D. F., Oliveira Battastini, A. M., & Eifler-Lima, V. L. (2015, May 4). Insights into ecto-5′-nucleotidase as a new target for cancer therapy: A medicinal chemistry study. *Current Medicinal Chemistry*, *22*(15), 1776–1792. https://doi.org/10.2174/0929867322666150408112615

Costea, T., Hudiţă, A., Ciolac, O.-A., Gălăţeanu, B., Ginghină, O., Costache, M., Ganea, C., & Mocanu, M.-M. (2018, November 28). Chemoprevention of colorectal cancer by dietary compounds. *International Journal of Molecular Sciences*, *19*(12), 3787. https://doi.org/10.3390/ijms19123787

Dal Bello, M. G., Filiberti, R. A., Alama, A., Orengo, A. M., Mussap, M., Coco, S., Vanni, I., Boccardo, S., Rijavec, E., Genova, C., Biello, F., Barletta, G., Rossi, G., Tagliamento, M., Maggioni, C., & Grossi, F. (2019, March 8). The role of CEA, CYFRA21-1 and NSE in monitoring tumor response to nivolumab in advanced non-small cell lung cancer (NSCLC) patients. *Journal of Translational Medicine*, *17*(1), 74. https://doi.org/10.1186/s12967-019-1828-0

Devlin, E. J., Denson, L. A., & Whitford, H. S. (2017, August). Cancer treatment side effects: A meta-analysis of the relationship between response expectancies and experience. *Journal of Pain and Symptom Management*, *54*(2), 245.e2–258.e2. https://doi.org/10.1016/j.jpainsymman.2017.03.017

Du, X., Li, D., Wang, G., Fan, Y., Li, N., Chai, L., Li, G., & Li, J. (2021, February). Chemoprotective effect of atorvastatin against benzo(a)pyrene-induced lung cancer via the inhibition of oxidative stress and inflammatory parameters. *Annals of Translational Medicine*, *9*(4), 355. https://doi.org/10.21037/atm-20-7770

Elumalai, P., Gunadharini, D. N., Senthilkumar, K., Banudevi, S., Arunkumar, R., Benson, C. S., Sharmila, G., & Arunakaran, J. (2012, November 30). Induction of apoptosis in human breast cancer cells by nimbolide through extrinsic and intrinsic pathway. *Toxicology Letters*, *215*(2), 131–142. https://doi.org/10.1016/j.toxlet.2012.10.008

Galluzzi, L., Buqué, A., Kepp, O., Zitvogel, L., & Kroemer, G. (2015, December 14). Immunological effects of conventional chemotherapy and targeted anticancer agents. *Cancer Cell*, *28*(6), 690–714. https://doi.org/10.1016/j.ccell.2015.10.012

Hanahan, D. (2022, January). Hallmarks of cancer: New dimensions. *Cancer Discovery*, *12*(1), 31–46. https://doi.org/10.1158/2159-8290.CD-21-1059

Hernandez-Boussard, T. M., & Hainaut, P. (1998, July). A specific spectrum of p53 mutations in lung cancer from smokers: Review of mutations compiled in the IARC p53 database. *Environmental Health Perspectives*, *106*(7), 385–391. https://doi.org/10.1289/ehp.98106385

Huang, L., Zhang, P., Duan, S., Shao, H., Gao, M., Zhang, Q., & Feng, F. (2019, August 14). The comparison of two mouse models of inflammation-related lung tumorigenesis induced by benzo(a)pyrene and lipopolysaccharide. *Experimental Animals*, *68*(3), 301–306. https://doi.org/10.1538/expanim.18-0159

Imtiaz, I., Schloss, J., & Bugarcic, A. (2024, January–February). Traditional and contemporary herbal medicines in management of cancer: A scoping review. *Journal of Ayurveda and Integrative Medicine*, *15*(1), Article 100904. https://doi.org/10.1016/j.jaim.2024.100904

Jenča, A., Mills, D. K., Ghasemi, H., Saberian, E., Jenča, A., Karimi Forood, A. M., Petrášová, A., Jenčová, J., Jabbari Velisdeh, Z., Zare-Zardini, H., & Ebrahimifar, M. (2024, September 10). Herbal therapies for cancer treatment: A review of phytotherapeutic efficacy. *Biologics: Targets & Therapy*, *18*, 229–255. https://doi.org/10.2147/BTT.S484068

Jia, L., Gao, F., Hu, G., Fang, Y., Tang, L., Wen, Q., Gao, N., Xu, H., & Qiao, H. (2023, December). A novel cytochrome P450 2E1 inhibitor Q11 is effective on lung cancer via regulation of the inflammatory microenvironment. *Advancement of Science (Weinh)*, *10*(35), Article e2303975. https://doi.org/10.1002/advs.202303975

Jung, M., Kim, S. H., Lee, Y. J., Hong, S., Kang, Y. A., Kim, S. K., Chang, J., Rha, S. Y., Kim, J. H., Kim, D. J., & Cho, B. C. (2011, July). Prognostic and predictive value of CEA and CYFRA 21–1 levels in advanced non-small cell lung cancer patients treated with gefitinib or erlotinib. *Experimental and Therapeutic Medicine*, *2*(4), 685–693. https://doi.org/10.3892/etm.2011.273

Kamaraj, S., Anandakumar, P., Jagan, S., Ramakrishnan, G., & Devaki, T. (2011, February). Hesperidin attenuates mitochondrial dysfunction during benzo(a)pyrene-induced lung carcinogenesis in mice. *Fundamental and Clinical Pharmacology*, *25*(1), 91–98. https://doi.org/10.1111/j.1472-8206.2010.00812.x

King, J. (1965). The hydrolases-acid and alkaline phosphatases. In D. Van (Ed.), *Practical clinical enzymology* (pp. 199–208). Nostrand Co.

Kolluri, S. K., Jin, U.-H., & Safe, S. (2017, July). Role of the aryl hydrocarbon receptor in carcinogenesis and potential as an anticancer drug target. *Archives of Toxicology*, *91*(7), 2497–2513. https://doi.org/10.1007/s00204-017-1981-2

Koukourakis, M. I., Giatromanolaki, A., Sivridis, E., Bougioukas, G., Didilis, V., Gatter, K. C., Harris, A. L., & Tumour and Angiogenesis Research Group. (2003, September 1). Lactate dehydrogenase-5 (LDH-5) overexpression in non-small-cell lung cancer tissues is linked to tumour hypoxia, angiogenic factor production and poor prognosis. *British Journal of Cancer*, *89*(5), 877–885. https://doi.org/10.1038/sj.bjc.6601205

Kryczka, J., Kryczka, J., Czarnecka-Chrebelska, K. H., & Brzeziańska-Lasota, E. (2021, August 18). Molecular mechanisms of chemoresistance induced by cisplatin in NSCLC cancer therapy. *International Journal of Molecular Sciences*, *22*(16), 8885. https://doi.org/10.3390/ijms22168885

Kuang, Z., Wang, J., Liu, K., Wu, J., Ge, Y., Zhu, G., Cao, L., Ma, X., & Li, J. (2024, September 5). Global, regional, and national burden of tracheal, bronchus, and lung cancer and its risk factors from 1990 to 2021: Findings from the global burden of disease study 2021. *EClinicalmedicine*, *75*, Article 102804. https://doi.org/10.1016/j.eclinm.2024.102804

Mahady, G. B. (2001, March). Global harmonization of herbal health claims. *The Journal of Nutrition*, *131*(3s), 1120S–1123S. https://doi.org/10.1093/jn/131.3.1120S

Matsumoto, H., Ando, S., Yoshimoto, E., Numano, T., Sultana, N., Fukamachi, K., Iinuma, M., Okuda, K., Kimura, K., & Suzui, M. (2022). Extracts of *Musa basjoo* induce growth inhibition and changes in the protein expression of cell cycle control molecules in human colorectal cancer cell lines. *Oncology Letters*, *23*(3), 99. https://doi.org/10.3892/ol.2022.13219

Maurya, A., Dwivedi, G. R., Darokar, M. P., & Srivastava, S. K. (2013, April). Antibacterial and synergy of clavine alkaloid lysergol and its derivatives against nalidixic acid-resistant *Escherichia coli*. *Chemical Biology and Drug Design*, *81*(4), 484–490. https://doi.org/10.1111/cbdd.12103

Mehler, A. H., Kornberg, A., Grisolia, S., & Ochoa, S. (1948). The enzymatic mechanism of oxidation-reductions between malate or isocitrate and pyruvate. *Journal of Biological Chemistry*, *174*(3), 961–977. https://doi.org/10.1016/S0021-9258(18)57306-3

Molina, R., Agusti, C., Filella, X., Jo, J., Joseph, J., Giménez, N., & Ballesta, A. M. (1994). Study of a new tumor marker, CYFRA 21-1, in malignant and nonmalignant diseases. *Tumour Biology*, *15*(6), 318–325. https://doi.org/10.1159/000217908

Moorthy, B., Chu, C., & Carlin, D. J. (2015, May). Polycyclic aromatic hydrocarbons: From metabolism to lung cancer. *Toxicological Sciences*, *145*(1), 5–15. https://doi.org/10.1093/toxsci/kfv040

Mota, P., Silva, H. C., Soares, M. J., Pego, A., Loureiro, M., Cordeiro, C. R., & Regateiro, F. J. (2015, May). Genetic polymorphisms of phase I and phase II metabolic enzymes as modulators of lung cancer susceptibility. *Journal of Cancer Research and Clinical Oncology*, *141*(5), 851–860. https://doi.org/10.1007/s00432-014-1868-z

Naveenkumar, C., Raghunandhakumar, S., Asokkumar, S., & Devaki, T. (2013, April). Baicalein abrogates reactive oxygen species (ROS)-mediated mitochondrial dysfunction during experimental pulmonary carcinogenesis *in vivo*. *Basic and Clinical Pharmacology and Toxicology*, *112*(4), 270–281. https://doi.org/10.1111/bcpt.12025

Nulton-Persson, A. C., & Szweda, L. I. (2001). Modulation of mitochondrial function by hydrogen peroxide. *Journal of Biological Chemistry*, *276*(26), 23357–23361. https://doi.org/10.1074/jbc.M100320200

Okamura, K., Takayama, K., Izumi, M., Harada, T., Furuyama, K., & Nakanishi, Y. (2013, April). Diagnostic value of CEA and CYFRA 21–1 tumor markers in primary lung cancer. *Lung Cancer*, *80*(1), 45–49. https://doi.org/10.1016/j.lungcan.2013.01.002

Patil, S., Dash, R. P., Anandjiwala, S., & Nivsarkar, M. (2012, October). Simultaneous quantification of berberine and lysergol by HPLC-UV: Evidence that lysergol enhances the oral bioavailability of berberine in rats. *Biomedical Chromatography*, *26*(10), 1170–1175. https://doi.org/10.1002/bmc.2674

Peppas, I., George, G., Sollie, S., Josephs, D. H., Hammar, N., Walldius, G., Karagiannis, S. N., & Van Hemelrijck, M. (2020, March). Association of serum immunoglobulin levels with solid cancer: A systematic review and meta-analysis. *Cancer Epidemiology, Biomarkers and Prevention*, *29*(3), 527–538. https://doi.org/10.1158/1055-9965.EPI-19-0953

Pratheeshkumar, P., Sreekala, C., Zhang, Z., Budhraja, A., Ding, S., Son, Y.-O., Wang, X., Hitron, A., Hyun-Jung, K., Wang, L., Lee, J.-C., & Shi, X. (2012, December). Cancer prevention with promising natural products: Mechanisms of action and molecular targets. *Anti-Cancer Agents in Medicinal Chemistry*, *12*(10), 1159–1184. https://doi.org/10.2174/187152012803833035

Rajendran, P., Jayakumar, T., Nishigaki, I., Ekambaram, G., Nishigaki, Y., Vetriselvi, J., & Sakthisekaran, D. (2013, June). Immunomodulatory effect of mangiferin in experimental animals with benzo(a)pyrene-induced lung carcinogenesis. *International Journal of Biomedical Science*, *9*(2), 68–74. https://doi.org/10.59566/IJBS.2013.9068

Rasmi, R. R., Sakthivel, K. M., & Guruvayoorappan, C. (2020, October). NF-κB inhibitors in treatment and prevention of lung cancer. *Biomedicine and Pharmacotherapy*, *130*, Article 110569. https://doi.org/10.1016/j.biopha.2020.110569

Ratovitski, E. A. (2017, April). Anticancer natural compounds as epigenetic modulators of gene expression. *Current Genomics*, *18*(2), 175–205. https://doi.org/10.2174/1389202917666160803165229

Reed, L. J., & Mukherjee, B. B. (1969). α-Ketoglutarate dehydrogenase complex from *Escherichia coli*. *Methods in Enzymology*, *113*, 55–61.

Rostock, M., Naumann, J., Guethlin, C., Guenther, L., Bartsch, H. H., & Walach, H. (2011, January 17). Classical homeopathy in the treatment of cancer patients—A prospective observational study of two independent cohorts. *BMC Cancer*, *11*, 19. https://doi.org/10.1186/1471-2407-11-19

Selvendiran, K., Thirunavukkarasu, C., Singh, J. P. V., Padmavathi, R., & Sakthisekaran, D. (2005, March). Chemopreventive effect of piperine on mitochondrial TCA cycle and phase-I and glutathione-metabolizing enzymes in benzo(a)pyrene induced lung carcinogenesis in Swiss albino mice. *Molecular and Cellular Biochemistry*, *271*(1–2), 101–106. https://doi.org/10.1007/s11010-005-5615-2

Sertić Milić, H., Franjević, A., Bubanović, G., Marušić, A., Nikolić, I., & Puljić, I. (2015, June). Size, edge, and stage of NSCLC determine the release of CYFRA 21-1 in bloodstream. *Wiener Klinische Wochenschrift*, *127*(11–12), 465–471. https://doi.org/10.1007/s00508-014-0678-2

Sharonov, G. V., Serebrovskaya, E. O., Yuzhakova, D. V., Britanova, O. V., & Chudakov, D. M. (2020). B cells, plasma cells and antibody repertoires in the tumour microenvironment. *Nature Reviews. Immunology*, *20*(5), 294–307. https://doi.org/10.1038/s41577-019-0257-x

Shi, L., Wang, L., Hou, J., Zhu, B., Min, Z., Zhang, M., Song, D., Cheng, Y., & Wang, X. (2015). Targeting roles of inflammatory microenvironment in lung cancer and metastasis. *Cancer Metastasis Reviews*, *34*(2), 319–331. https://doi.org/10.1007/s10555-015-9570-4

Siegel, R. L., Miller, K. D., & Jemal, A. (2018, January). Cancer statistics, 2018. *CA: A Cancer Journal for Clinicians*, *68*(1), 7–30. https://doi.org/10.3322/caac.21442

Singh, S., Sharma, B., Kanwar, S. S., & Kumar, A. (2016, November 8). Lead phytochemicals for anticancer drug development. *Frontiers in Plant Science*, *7*, 1667. https://doi.org/10.3389/fpls.2016.01667

Stockley, R. A., Shaw, J., Whitfield, A. G., Whitehead, T. P., Clarke, C. A., & Burnett, D. (1986). Effect of cigarette smoking, pulmonary inflammation, and lung disease on concentrations of

carcinoembryonic antigen in serum and secretions. *Thorax*, *41*(1), 17–24. https://doi.org/10.1136/thx.41.1.17

Tan, Z., Xue, H., Sun, Y., Zhang, C., Song, Y., & Qi, Y. (2021, May 17). The role of tumor inflammatory microenvironment in lung cancer. *Frontiers in Pharmacology*, *12*, Article 688625. https://doi.org/10.3389/fphar.2021.688625

Wang, J. J., Lei, K. F., & Han, F. (2018, June). Tumor microenvironment: Recent advances in various cancer treatments. *European Review for Medical and Pharmacological Sciences*, *22*(12), 3855–3864. https://doi.org/10.26355/eurrev_201806_15270

Wang, L., Kong, W., Liu, B., & Zhang, X. (2018, August). Proliferating cell nuclear antigen promotes cell proliferation and tumorigenesis by up-regulating STAT3 in non-small cell lung cancer. *Biomedicine and Pharmacotherapy*, *104*, 595–602. https://doi.org/10.1016/j.biopha.2018.05.071

Wang, S., Zang, W., Yang, Y., Zhang, Q., Zhao, M., Gao, Z., Li, G., Meng, Q., Liu, Q., & Zheng, X. (2013, September). Tanshinone IIA and baicalin inhibiting the formation of benzo[*a*]pyrene and benzo[*a*]pyrene induced cytotoxicity: Correlation with scavenging free radical. *Environmental Toxicology and Pharmacology*, *36*(2), 403–410. https://doi.org/10.1016/j.etap.2013.05.003

Wei, J.-R., Dong, J., & Li, L. (2020, July 8). Cancer-associated fibroblasts-derived gamma-glutamyltransferase 5 promotes tumor growth and drug resistance in lung adenocarcinoma. *Aging*, *12*(13), 13220–13233. https://doi.org/10.18632/aging.103429

Yuan, H., Guo, Z., & Luo, T. (2017). Synthesis of (+)-lysergol and its analogues to assess serotonin receptor activity. *Organic Letters*, *19*(3), 624–627. https://doi.org/10.1021/acs.orglett.6b03779

Zhang, B., Tornmalm, J., Widengren, J., Vakifahmetoglu-Norberg, H., & Norberg, E. (2017, July 5). Characterization of the role of the malate dehydrogenases to lung tumor cell survival. *Journal of Cancer*, *8*(11), 2088–2096. https://doi.org/10.7150/jca.19373

Zhang, Q., Zhu, B., & Li, Y. (2017, February 2). Resolution of cancer-promoting inflammation: A new approach for anticancer therapy. *Frontiers in Immunology*, *8*, 71. https://doi.org/10.3389/fimmu.2017.00071

Zimta, A.-A., Cenariu, D., Irimie, A., Magdo, L., Nabavi, S. M., Atanasov, A. G., & Berindan-Neagoe, I. (2019, November 8). The role of Nrf2 activity in cancer development and progression. *Cancers*, *11*(11), 1755. https://doi.org/10.3390/cancers11111755

Zuo, J., Brewer, D. S., Arlt, V. M., Cooper, C. S., & Phillips, D. H. (2014, October 8). Benzo pyrene-induced DNA adducts and gene expression profiles in target and non-target organs for carcinogenesis in mice. *BMC Genomics*, *15*(1), 880. https://doi.org/10.1186/1471-2164-15-880